Modeling Three-Dimensional Morse and Morse-Smale Complexes

Lidija Čomić, Leila De Floriani, Federico Iuricich

Abstract

Morse and Morse-Smale complexes have been recognized as a suitable tool for modeling the topology of a manifold M through a decomposition of M induced by a scalar field f defined over M. We consider here the problem of representing, constructing and simplifying Morse and Morse-Smale complexes in 3D. We first describe and compare two data structures for encoding 3D Morse and Morse-Smale complexes. We describe, analyze and compare algorithms for computing such complexes. Finally, we consider the simplification of Morse and Morse-Smale complexes by applying coarsening operators on them, and we discuss and compare the coarsening operators on Morse and Morse-Smale complexes described in the literature.

1 Introduction

Topological analysis of discrete scalar fields is an active research field in computational topology. The available data sets defining the fields are increasing in size and in complexity. Thus, the definition of compact topological representations for scalar fields is a first step in building analysis tools capable of analyzing effectively large data sets. In the continuous case, Morse and Morse-Smale complexes have been recognized as convenient and theoretically well founded representations for modeling both the topology of the manifold domain M, and the behavior of a scalar

Lidija Čomić
Faculty of Engineering, University of Novi Sad, Trg D. Obradovića 6, Novi Sad, Serbia, e-mail: comic@uns.ac.rs

Leila De Floriani
Department of Computer Science, University of Genova, via Dodecaneso 35, Genova, Italy, e-mail: deflo@disi.unige.it

Federico Iuricich
Department of Computer Science, University of Genova, via Dodecaneso 35, Genova, Italy, e-mail: federico.iuricich@unige.it

field f over M. They segment the domain M of f into regions associated with critical points of f, which encode the features of both M and f.

Morse and Morse-Smale complexes have been introduced in computer graphics for the analysis of 2D scalar fields [EHZ01, BEHP03], and specifically for terrain modeling and analysis, where the domain is a region in the plane, and the scalar field is the elevation function [TIKU95, EDP$^+$03]. Recently, Morse and Morse-Smale complexes have been considered as a tool to analyze also 3D functions [EHNP03, GNP$^+$05]. They are used in scientific visualization, where data are obtained through measurements of scalar field values over a volumetric domain, or through simulation, such as the analysis of mixing fluids [BWP$^+$10]. With an appropriate selection of the scalar function, Morse and Morse-Smale complexes are also used for segmenting molecular models to detect cavities and protrusions, which influence interactions between proteins [CCL03, NWB$^+$06]. Morse complexes of the distance function have been used in shape matching and retrieval.

Scientific data, obtained either through measurements or simulation, is usually represented as a discrete set of vertices in a 2D or 3D domain M, together with function values given at those vertices. Algorithms for extracting an approximation of Morse and Morse-Smale complexes from a sampling of a (continuous) scalar field on the vertices of a simplicial complex Σ triangulating M have been extensively studied in 2D [TIKU95, BS98, EHZ01, BEHP04, Pas04, CCL03, DDM03]. Recently, some algorithms have been proposed for dealing with scalar data in higher dimensions [EHNP03, GNPH07, GBHP08, EJ09, ČomićDI10].

Although Morse and Morse-Smale complexes represent the topology of M and the behavior of f in a much more compact way than the initial data set at full resolution, simplification of these complexes is a necessary step for the analysis of noisy data sets. Simplification is achieved by applying the *cancellation operator* on f [Mat02], and on the corresponding Morse and Morse-Smale complexes. In 2D [TIKU95, EHZ01, BEHP04, Wol04, GNP$^+$05], a cancellation eliminates critical points of f, reduces the incidence relation on the Morse complexes, and eliminates cells from the Morse-Smale complexes. In higher dimensions, surprisingly, a cancellation may introduce cells in the Morse-Smale complex, and may increase the mutual incidences among cells in the Morse complex.

Simplification operators, together with their inverse refinement ones, form a basis for the definition of a multi-resolution representation of Morse and Morse-Smale complexes, crucial for the analysis of the present-day large data sets. Several approaches for building such multi-resolution representations in 2D have been proposed [BEHP04, BPH05, DDVM07]. In higher dimensions, such hierarchies are based on a progressive simplification of the initial full-resolution model.

Here, we briefly review the well known work on extraction, simplification, and multi-resolution representation of Morse and Morse-Smale complexes in 2D. Then, we review in greater detail and compare the extension of this work to three and higher dimensions. Specifically, we compare the data structure introduced in [GNP$^+$06] for encoding 3D Morse-Smale complexes with a 3D instance of the dimension-independent data structure proposed in [ČomićDI10] for encoding Morse complexes. We review the existing algorithms for the extraction of an approximation of Morse and Morse-Smale complexes in three and higher dimensions. Finally, we review and compare the two existing approaches in the literature to the simplification of the topological representation given by Morse and Morse-Smale complexes, without changing the topology of M. The first approach [GNP$^+$05] implements a cancellation operator defined for Morse functions [Mat02] on the corresponding Morse-Smale complexes. The second approach [ČomićD11] implements only a well-behaved subset of cancellation operators, which still forms a basis for the set of operators that modify Morse and Morse-Smale complexes on M in a topologically consistent manner. These operators also form a basis for the definition of a multi-resolution representation of Morse and Morse-Smale complexes.

2 Background Notions

We review background notions on Morse theory and Morse complexes for C^2 functions, and some approaches to discrete representations for Morse and Morse-Smale complexes.

Morse theory captures the relationships between the topology of a manifold M and the critical points of a scalar (real-valued) function f defined on M [Mat02, Mil63]. An *n-manifold* M without boundary is a topological space in which each point p has a neighborhood homeomorphic to $\mathbb{R}^n$. In an n-manifold with boundary, each point p has a neighborhood homeomorphic to $\mathbb{R}^n$ or to a half-space $\mathbb{R}^n_+ = \{(x_1, x_2, ..., x_n) \in \mathbb{R}^n : x_n \geq 0\}$ [Kel55].

Let f be a C^2 real-valued function (scalar field) defined over a manifold M. A point $p \in M$ is a *critical point* of f if and only if the gradient $\nabla f = (\frac{\partial f}{\partial x_1}, ..., \frac{\partial f}{\partial x_n})$ (in some local coordinate system around p) of f vanishes at p. Function f is said to be a *Morse function* if all its critical points are non-degenerate (the Hessian matrix $Hess_p f$ of the second derivatives of f at p is non-singular). For a Morse function f, there is a neighborhood of each critical point $p = (p_1, p_2, ..., p_n)$ of f, in which $f(x_1, x_2, \ldots, x_n) = f(p_1, p_2, ..., p_n) - x_1^2 - \ldots - x_i^2 + x_{i+1}^2 + \ldots + x_n^2$ [Mil63]. The number i is equal to the number of negative eigenvalues of $Hess_p f$, and is called the *index* of critical point p. The corresponding eigenvectors point in the directions in which f is decreasing. If the index of p is i, $0 \leq i \leq n$, p is called an *i-saddle*. A 0-saddle is called a *minimum*, and an n-saddle is called a *maximum*. Figure 1 illustrates a neighborhood of a critical point in three dimensions.

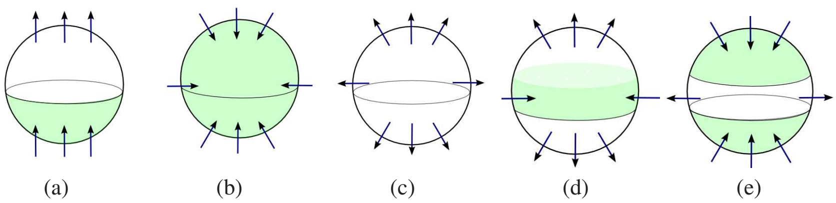

Fig. 1 Classification of non-degenerate critical points in the 3D case. Arrowed lines represent integral lines, green regions contain points with the lower function value. (a) A regular point, (b) a local maximum, (c) a local minimum, (d) a 1-saddle and (e) a 2-saddle.

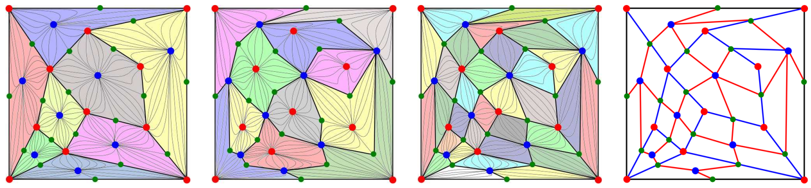

Fig. 2 A portion of (a) a descending Morse complex; (b) the dual ascending Morse complex; (c) the Morse-Smale complex; (d) the 1-skeleton of the Morse-Smale complex in 2D.

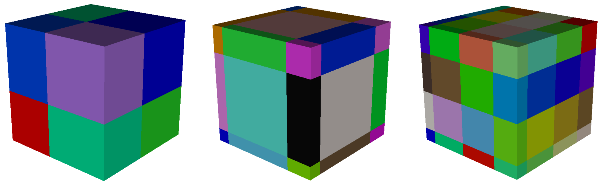

Fig. 3 A portion of (a) a descending and (b) ascending 3D Morse complex, and (c) the corresponding Morse-Smale complex, defined by a function $f(x,y,z) = \sin x + \sin y + \sin z$.

An *integral line* of a function f is a maximal path that is everywhere tangent to the gradient ∇f of f. It follows the direction in which the function has the maximum increasing growth. Two integral lines are either disjoint, or they are the same. Each integral line starts at a critical point of f, called its *origin*, and ends at another critical point, called its *destination*. Integral lines that converge to a critical point p of index i cover an i-cell called the *stable (descending) cell* of p. Dually, integral lines that originate at p cover an $(n-i)$-cell called the *unstable (ascending) cell* of p. The descending cells (or manifolds) are pairwise disjoint, they cover M, and the boundary of every cell is a union of lower-dimensional cells. Descending cells decompose M into a cell complex Γ_d, called the *descending Morse complex* of f on M. Dually, the ascending cells form the *ascending Morse complex* Γ_a of f on M. Figure 2 (a) and (b) and Figure 3 (a) and (b) show an example of a descending and dual ascending Morse complex in 2D and 3D, respectively.

A Morse function f is called a *Morse-Smale function* if and only if each non-empty intersection of a descending and an ascending cell is transversal. This means that each connected component of the intersection (if it exists) of the descending i-cell of a critical point p of index i, and the ascending $(n-j)$-cell of a critical point q of index j, $i \geq j$, is an $(i-j)$-cell. The connected components of the intersection of descending and ascending cells of a Morse-Smale function f decompose M into a *Morse-Smale complex*. If f is a Morse-Smale function, then there is no integral line connecting two different critical points of f of the same index. Each 1-saddle is connected to exactly two (not necessarily distinct) minima, and each $(n-1)$-saddle is connected to exactly two (not necessarily distinct) maxima. The 1-skeleton of the

Morse-Smale complex is the subcomplex composed of 0-cells and 1-cells. It plays an important role in the applications, as it is often used as a graph-based representation of the Morse and Morse-Smale complexes. Figure 2 (c) in 2D and Figure 3 (c) in 3D illustrate the Morse-Smale complex corresponding to the ascending and descending Morse complexes of Figure 2 (a) and (b) and Figure 3 (a) and (b), respectively. Figure 2 (d) shows the 1-skeleton of the Morse-Smale complex in Figure 2 (c).

The first approaches to develop a discrete version of Morse theory aimed at a generalization of the notion of critical points (maxima, minima, saddles) to the case of a scalar field f defined on the vertices of a simplicial complex Σ triangulating a 2D manifold (surface) M. This generalization was first done in [Ban70] in 2D, and has been used in many algorithms [TIKU95, EHZ01, NGH04]. The classification of critical points is done based on the f value at a vertex p, and the vertices in the link $Lk(p)$ of p. The link $Lk(p)$ of each vertex p of Σ can be decomposed into three sets, $Lk^+(p)$, $Lk^-(p)$, and $Lk^\pm(p)$. The *upper link* $Lk^+(p)$ consists of the vertices $q \in Lk(p)$ with higher f value than $f(p)$, and of edges connecting such vertices. The *lower link* $Lk^-(p)$ consists of the vertices with lower f value than $f(p)$, and of edges connecting such vertices. The set $Lk^\pm(p)$ consists of *mixed edges* in $Lk(p)$, each connecting a vertex with higher f value than $f(p)$ to a vertex with lower f value than $f(p)$. If the lower link $Lk^-(p)$ is empty, then p is a minimum. If the upper link $Lk^+(p)$ is empty, then p is a maximum. If the cardinality of $Lk^\pm(p)$ is $2+2m(p)$, then p is a saddle with multiplicity $m(p) \geq 1$. Otherwise, p is a regular point. The classification of a vertex based on these rules is illustrated in Figure 4.

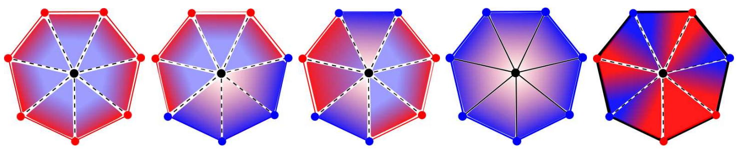

Fig. 4 The classification of a vertex based on the function values of the vertices in its link (minimum, regular point, simple saddle, maximum, 2-fold saddle). The lower link Lk^- is marked in blue, the upper link is red.

There have been basically two approaches in the literature to extend the results of Morse theory and represent Morse and Morse-Smale complexes in the discrete case. One approach, called *Forman theory* [For98], considers a discrete Morse function (*Forman* function) defined on all cells of a cell complex. The other approach, introduced in [EHZ01] in 2D, and in [EHNP03] in 3D, provides a combinatorial description, called a *quasi-Morse-Smale complex*, of the Morse-Smale complex of a scalar field f defined at the vertices of a simplicial complex.

The main purpose of Forman theory is to develop a discrete setting in which almost all the main results from smooth Morse theory are valid. This goal is achieved by considering a function F defined on all cells, and not only on the vertices, of a cell complex Γ. Function F is a Forman function if for any i-cell σ, all the $(i-1)$-cells on the boundary of σ have a lower F value than $F(\sigma)$, and all the $(i+1)$-cells in the co-boundary of σ have a higher F value than $F(\sigma)$, with at most one exception. If there is such an exception, it defines a pairing of cells of Γ, called a *discrete* (or *Forman*) *gradient vector field* V. Otherwise, i-cell σ is a critical cell of index i. Similar to the smooth Morse theory, critical cells of a Forman function can be cancelled in pairs. In the example in Figure 5 (a), a Forman function F defined on a 2D simplicial complex is illustrated. Each simplex is labelled by its function value. Figure 5 (b) shows the Forman gradient vector field defined by Forman function F in Figure 5 (a). Vertex labelled 0 and edge labelled 6 are critical simplexes of F.

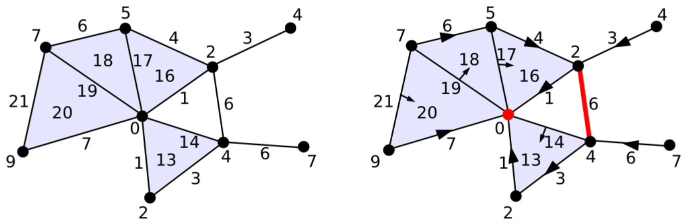

(a) (b)

Fig. 5 (a) Forman function F defined on a 2D simplicial complex, and (b) the corresponding discrete gradient vector field. Each simplex is labelled by its F value.

Forman theory finds important applications in computational topology, computer graphics, scientific visualization, molecular shape analysis, and geometric modeling. In [LLT04], Forman theory is used to compute the homology of a simplicial complex with manifold domain, while in [CCL03], it is used for segmentation of molecular surfaces. Forman theory can be used to compute Morse and Morse-Smale complexes of a scalar field f defined on the vertices of a simplicial or cell complex, by extending scalar field f to a Forman function F defined on all cells of the complex [KKM05, GBHP08, RWS11, ČomićMD11].

The notion of a quasi-Morse-Smale complex in 2D and 3D has been introduced in [EHZ01, EHNP03] with the aim of capturing the combinatorial structure of a Morse-Smale complex of a Morse-Smale function f defined over a manifold M. In 2D, a quasi-Morse-Smale complex is defined as a complex whose 1-skeleton is a tripartite graph, since the set of its vertices is partitioned into subsets corresponding to critical points (minima, maxima, and saddles). A vertex corresponding to a saddle has four incident edges, two of which connect it to vertices corresponding to minima, and the other two connect it to maxima. Each region (2-cell of the complex) is a quadrangle whose vertices are a saddle, a minimum, a saddle, and a maximum. In 3D, vertices of a quasi-Morse-Smale complex are partitioned into four sets corresponding to critical points. Each vertex corresponding to a 1-saddle is the extremum vertex of two edges connecting it to two vertices corresponding to minima, and dually for 2-saddles and maxima. Each 2-cell is a quadrangle, and there are exactly four 2-cells incident in each edge connecting a vertex corresponding to a 1-saddle to a vertex corresponding to a 2-saddle.

3 Related Work

In this section, we review related work on topological representations of 2D scalar fields based on Morse or Morse-Smale complexes. We concentrate on three topics relevant to the work presented here, namely: computation, simplification and multi-resolution representation of Morse and Morse-Smale complexes.

Several algorithms have been proposed in the literature for decomposing the domain of a 2D scalar field f into an approximation of a Morse or a Morse-Smale complex. For a review of the work in this area see [BFF$^+$08]. Algorithms for decomposing the domain M of field f into an approximation of a Morse, or of a Morse-Smale, complex can be classified as *boundary-based* [TIKU95, BS98, EHZ01, BEHP04, Pas04], or *region-based* [CCL03, DDM03]. Boundary-based algorithms trace the integral lines of f, which start at saddle points and converge to minima and maxima of f. Region-based methods grow the 2D cells corresponding to minima and maxima of f, starting from those critical points.

One of the major issues that arise when computing a representation of a scalar field as a Morse, or as a Morse-Smale, complex is the over-segmentation due to the presence of noise in the data sets. Simplification algorithms eliminate less significant features from these complexes. Simplification is achieved by applying an operator called *cancellation*, defined in Morse theory [Mat02]. It transforms a Morse function f into Morse function g with fewer critical points. Thus, it transforms a Morse-Smale complex into another, with fewer vertices, and it transforms a Morse complex into another, with fewer cells. It enables also the creation of a hierarchical representation. A cancellation in 2D consists of collapsing a maximum-saddle pair into a maximum, or a minimum-saddle pair into a minimum. Cancellation is performed in the order usually determined by the notion of *persistence*. Intuitively, persistence measures the importance of the pair of critical points to be cancelled, and is equal to the absolute difference in function values between the paired critical points [EHZ01]. In 2D Morse-Smale complexes, the cancellation operator has been investigated in [TIKU95, EHZ01, BEHP04, Wol04]. In [DDVM07], the cancellation operator in 2D has been extended to functions that may have multiple saddles and macro-saddles (saddles that are connected to each other).

Due to the large size and complexity of available scientific data sets, a multi-resolution representation is crucial for their interactive exploration. There have been several approaches in the literature to multi-resolution representation of the topology of a scalar field in 2D [BEHP04, BPH05, DDVM07]. The approach in [BEHP04] is based on a hierarchical representation of the 1-skeleton of a Morse-Smale complex, generated through the cancellation operator. It considers the 1-skeleton at full resolution and generates a sequence of simplified representations of the complex by repeatedly applying a cancellation operator. In [BPH05], the inverse anticancellation operator to the cancellation operator in [BEHP04] has been defined. It enables a definition of a dependency relation between refinement modifications, and a creation of a multi-resolution model for 2D scalar fields. The method in [DDVM07] creates a hierarchy of graphs (generalized critical nets), obtained as a 1-skeleton of an overlay of ascending and descending Morse complexes of a function with multiple saddles and saddles that are connected to each other. Hierarchical watershed approaches have been developed to cope with the increase in size of both 2D and 3D images [Beu94].

There have been two attempts in the literature to couple the multi-resolution topological model provided by Morse-Smale complexes with the multi-resolution model of the geometry of the underlying simplicial mesh. The approach in [BEHP04] first creates a hierarchy of Morse-Smale complexes by applying cancellation operators to the full-resolution complex, and then, by Laplacian smoothing, it constructs the smoothed function corresponding to the simplified topology. The approach in [DDMV10] creates the hierarchy by applying half-edge contraction operator, which simplifies the geometry of the mesh. When necessary, the topological representation corresponding to the simplified coarser mesh is also simplified. The data structure encoding the geometrical hierarchy of the mesh, and the data structure encoding the topological hierarchy of the critical net are interlinked. The hierarchical critical net is used as a topological index to query the hierarchical representation of the geometry of the simplicial mesh.

4 Representing Three-Dimensional Morse and Morse-Smale Complexes

In this section, we describe and compare two data structures for representing the topology and geometry of a scalar field f defined over the vertices of a simplicial complex Σ with manifold domain in 3D. The topology of scalar field f (and of its domain Σ) is represented in the form of Morse and Morse-Smale complexes. The two data structures encode the topology of the complexes in essentially the same way, namely in the form of a graph, usually called an *incidence graph*. The difference between the two data structures is in the way they encode the geometry: the data structure in [ČomićDI10] (its 3D instance) encodes the geometry of the 3-cells of the descending and ascending complexes; the data structure in [GNP$^+$06] encodes the geometry of the ascending and descending 3-, 2- and 0-cells in the descending and ascending Morse complexes, and that of the 1-cells in the Morse-Smale complexes.

4.1 A Dimension-Independent Compact Representation for Morse Complexes

The incidence-based representation proposed in [ČomićDI10] is a dual representation for the ascending and the descending Morse complexes Γ_a and Γ_d. The topology of both complexes is represented by encoding the immediate boundary and co-boundary relations of the cells in the two complexes in the form of a *Morse Incidence Graph (MIG)*. The Morse incidence graph provides also a combinatorial representation of the 1-skeleton of a Morse-Smale complex. In the discrete case the Morse incidence graph is coupled with a representation for the underlying simplicial mesh Σ. The two representations (of the topology and of the geometry) are combined into the *incidence-based data structure*, which is completely dimension-independent. This makes it suitable also for encoding Morse complexes in higher dimensions, e.g. 4D Morse complexes representing time-varying 3D scalar fields.

A *Morse Incidence Graph (MIG)* is a graph $\mathbb{G} = (\mathbb{N}, \mathbb{A})$ in which:

- the set of nodes $\mathbb{N}$ is partitioned into $n+1$ subsets $\mathbb{N}_0$, $\mathbb{N}_1$,...,$\mathbb{N}_n$, such that there is a one-to-one correspondence between the nodes in $\mathbb{N}_i$ (*i-nodes*) and the i-cells of Γ_d, (and thus the $(n-i)$-cells of Γ_a);
- there is an arc joining an i-node p with an $(i+1)$-node q if and only if the corresponding cells p and q differ in dimension by one, and p is on the boundary of q in Γ_d, (and thus q is on the boundary of p in Γ_a);
- each arc connecting an i-node p to an $(i+1)$-node q is labelled by the number of times i-cell p (corresponding to i-node p) in Γ_d is incident to $(i+1)$-cell q (corresponding to $(i+1)$-node q) in Γ_d.

In Figure 6, we illustrate a 2D ascending complex, and the corresponding incidence graph of function $f(x,y) = \sin x + \sin y$. In the ascending complex, cells labeled p are 2-cells (corresponding to minima), cells labeled r are 1-cells (corresponding to saddles), and cells labeled q are 0-cells (corresponding to maxima).

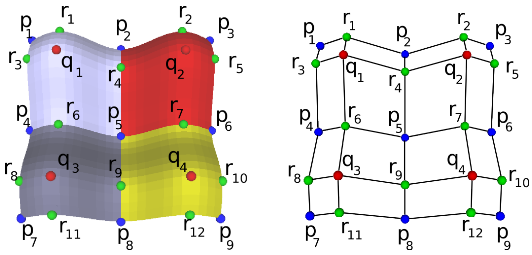

Fig. 6 (a) Ascending 2D Morse complex of function $f(x,y) = \sin x + \sin y$ and (b) the corresponding Morse incidence graph.

The data structure for encoding the *MIG* $\mathbb{G} = (\mathbb{N}, \mathbb{A})$ is illustrated in Figure 7. The nodes and the arcs of $\mathbb{G}$ are encoded as two lists. Recall that each node in the graph corresponds to a critical point p of f and to a vertex in the Morse-Smale complex. When p is an extremum, the corresponding element in the list of nodes contains three fields, G_0, G_n and A. The geometry of the extremum (its coordinates) is stored in field G_0, and the geometry of the associated n-cell (ascending n-cell of a minimum, or a descending n-cell of a maximum), which is the list of n-simplexes forming the corresponding n-cell in the ascending or descending complex, is stored in field G_n. The list of the pointers to the arcs incident in the extremum is stored in field A. If p is a maximum (n-saddle), these arcs connect p to $(n-1)$-saddles. If p is a minimum (0-saddle), they connect p to 1-saddles. When p is not an extremum, element in the node list contains fields G_0, A_1 and A_2.The geometry of i-saddle p (its coordinates) is stored in field G_0. A list of pointers to the arcs connecting i-saddle p to $(i+1)$-saddles and to $(i-1)$-saddles is stored in fields A_1 and A_2, respectively.

Each arc in the *MIG* corresponds to integral lines connecting two critical points of f, which are the endpoints of the arc. Each element in the list of arcs has three fields, CP_1, CP_2 and L. If the arc connects an i-saddle to an $(i+1)$-saddle, then CP_1 is a pointer to the i-saddle, and CP_2 is a pointer to the $(i+1)$-saddle. The label of the arc (its multiplicity) is stored in field L.

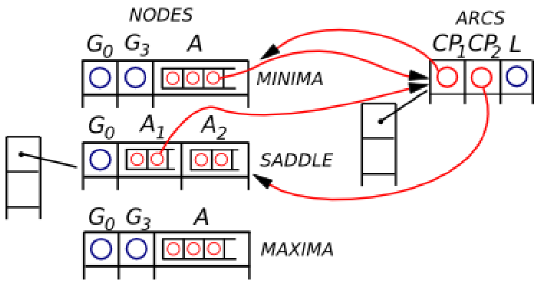

Fig. 7 Dimension-independent data structure for storing the incidence graph. The nodes corresponding to i-saddles are stored in lists, as are the arcs. Each element in the list of nodes stores the geometry of the corresponding critical point, and the list of pointers to arcs incident in the node. A node corresponding to an extremum stores also a list of pointers to the n-simplexes in the corresponding n-cell associated with the extremum. Each element in the list of arcs stores pointers to its endpoints, and a label indicating its multiplicity.

The manifold simplicial mesh Σ discretizing the graph of the scalar field is encoded in a data structure which generalizes the indexed data structure with adjacencies, commonly used for triangular and tetrahedral meshes [DH07]. It stores the 0-simplexes (vertices) and n-simplexes explicitly plus some topological relations, namely: for every n-simplex σ, the $n+1$ vertices of σ; for every n-simplex σ, the $n+1$ n-simplexes which share an $(n-1)$-simplex with σ; for every 0-simplex, one n-simplex incident in it.

The vertices and n-simplexes are stored in two arrays. In the array of vertices, for each vertex its Cartesian coordinates are encoded, and the field value associated with it. In the array of n-simplexes, with each n-simplex σ of the underlying mesh Σ the indexes of the minimum and of the maximum node in $\mathbb{G}$ are associated such that σ belongs to the corresponding ascending n-cell of the minimum, and descending n-cell of the maximum.

The resulting data structure is completely dimension-independent, since both the encoding of the mesh and of the graph are independent of the dimension of the mesh and of the algorithm used for the extraction of Morse complexes. The only geometry is the one of the maximal cells in the two Morse complexes, from which the geometry of all the other cells of the Morse complexes can be extracted. The geometry of these cells can be computed iteratively, from higher to lower dimensions, by searching for the k-simplexes that are shared by $(k+1)$-simplexes belonging to different $(k+1)$-cells.

The incidence-based data structure encodes also the topology of the Morse-Smale complex. The arcs in the graph (i.e., pairs of nodes connected through the arc) correspond to 1-cells in the Morse-Smale complex. Similarly, pairs of nodes connected through a path of length k correspond to k-cells in the Morse-Smale complex. The geometry of these cells can be computed from the geometry of the cells in the Morse complex through intersection. For example, the intersection of ascending n-cells corresponding to minima and descending n-cells corresponding to maxima defines n-cells in the Morse-Smale complex.

4.2 A Dimension-Specific Representation for 3D Morse-Smale Complexes

In [GNP+06] a data structure for 3D Morse-Smale complexes is presented. The topology of the Morse-Smale complex (actually of its 1-skeleton) is encoded in a data structure equivalent to the Morse incidence graph. The geometry is referred to from the elements of the graph, arcs and nodes. We illustrate this data structure in Figure 8.

The data structure encodes the nodes and arcs of the incidence graph in two arrays. Each element in the list of nodes has four fields, G_0, TAG, G_2/G_3 and A. The geometry (coordinates) of the corresponding critical point is stored in field G_0. The index of the critical point is stored in field TAG. A reference to the geometry of the associated Morse cell (depending on the index of p) is stored in field G_2/G_3: a descending 3-cell is associated with a maximum; an ascending 3-cell is associated with a minimum; a descending 2-cell is associated with a 2-saddle; an ascending 2-cell is associated with a 1-saddle. A pointer to an arc incident in the node (the first one in the list of such arcs) is stored in field A. Thus, the geometry of 0-, 2-, and 3-cells in the Morse complexes is referenced from the nodes.

Each element in the list of arc has five fields, G_1,CP_1, CP_2, A_1 and A_2. The geometry of the integral line (corresponding to a 1-cell in the Morse-Smale complex) encoded by the arc is stored in field G_1. The pointers to the nodes connected by the arc are stored in fields CP_1 and CP_2. Fields A_1 and A_2 contain pointers to the next arcs incident in nodes pointed at by CP_1 and CP_2, respectively.

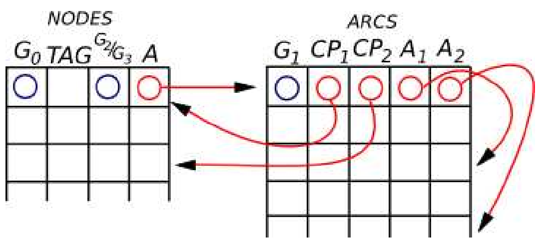

Fig. 8 Dimension-specific data structure for storing the incidence graph. Nodes and arcs are stored in lists. Each element in the list of nodes stores the geometry of the corresponding critical point, tag indicating the index of the critical point, geometry of the associated 2- or 3-cell in the Morse complex, and a pointer to one incident arc. Each element in the list of arcs stores the geometry of the arc, two pointers to its endpoints, and two pointers to the next arcs incident in the two endpoints.

The data structure in [GNP+06] is dimension-specific, because it represents 0-cells, 2-cells and 3-cells of the Morse complexes in the nodes, and 1-cells of the Morse-Smale complexes in the arcs of the incidence graph. The descending 1-cells in the Morse complex can be obtained as union of (the geometry associated with) two arcs incident in a node corresponding to a 1-saddle, and ascending 1-cells can be obtained as union of two arcs incident in a 2-saddle.

4.3 Comparison

The data structure in [GNP+06] encodes the combinatorial representation of the 1-skeleton of the Morse-Smale complex, which is equivalent to the encoding of the Morse incidence graph in [ČomićDI10].

Let us denote as n the number of nodes, and as a the number of arcs in the incidence graph. Both data structures encode the nodes and arcs of G in lists. Thus, the cost of maintaining those lists in both data structures is $n+a$. In the incidence-based representation in [ČomićDI10], for each arc there are two pointers pointing to it (one from each of its endpoints) and there are two pointers from the arc to its two endpoints. Thus, storing the connectivity information of the Morse incidence graph requires $4a$ pointers in [ČomićDI10]. In the data structure in [GNP+06], for each node there is a pointer to one arc incident in it, and for each arc there are four pointers, two pointing to its endpoints, and two pointing to the next arcs incident in the endpoints. This gives a total cost of $n+4a$ pointers for storing the connectivity information of the graph in [GNP+06].

The difference between the two representations is how geometry is encoded. In the 3D instance of the incidence-based data structure, only the list of tetrahedra forming the ascending and descending 3-cells are encoded. This leads to a cost of twice the number of tetrahedra in the simplicial mesh Σ since each tetrahedron belongs to exactly one ascending and one descending 3-cell. The data structure in [GNP+06] encodes the geometry of the arcs (i.e., the 1-cells in the Morse-Smale complex), the geometry of the ascending and descending 3-cells in the Morse complexes, associated with the nodes encoding the extrema, and the geometry of the ascending and descending 2-cells in the Morse complexes associated with the nodes encoding the saddles. We cannot evaluate precisely the storage cost of this latter data structure, since in [GNP+06] it is not specified how the underlying geometry is encoded. However, the combinatorial part of the two data structures has almost the same cost. Thus, it is clear that the incidence-based representation is more compact since it encodes fewer geometric information.

5 Algorithms for Building 3D Morse and Morse-Smale Complexes

In this section, we describe and compare algorithms for extracting Morse and Morse-Smale complexes from a scalar field f defined on the vertices of a manifold simplicial mesh Σ in 3D. Similarly to the 2D case, extraction and classification of critical points is a usual preprocessing step. An algorithm performing this task is proposed in [EHNP03]. For each vertex p of Σ, the lower link $Lk^-(p)$ of p is considered. It consists of the vertices q in the link $Lk(p)$ of p such that $f(q) < f(p)$, and of the simplexes of $Lk(p)$ defined by these vertices. Vertex p is classified as a minimum if its lower link is empty. It is classified as a maximum if its lower link is the same as $Lk(p)$. Otherwise, p is classified based on the Betti numbers of $Lk^-(p)$ as a critical point composed of multiple 1- and 2-saddles. Intuitively, the Betti numbers β_0 and β_1 of $Lk^-(p)$ count the number of connected components and holes in $Lk^-(p)$, respectively.

The algorithms presented here can be classified, according to the approach they use, as *region-based* [GNPH07, ČomićDI10], *boundary-based* [EHNP03, EJ09], or *based on Forman theory* [KKM05, GBHP08, RWS11]. Region-based algorithms extract only the minima and maxima of f, and do not explicitly extract saddle points. Boundary-based algorithms [EHNP03, EJ09] first extract and classify critical points of f (minima, maxima, and multiple 1- and 2-saddles) in the preprocessing step (using the method in [EHNP03]), and then compute the ascending and descending 1-cells and 2-cells associated with saddles. The algorithms in [KKM05, GBHP08, RWS11] construct a Forman gradient vector field V and its critical cells starting from a scalar field f.

The output of the algorithm in [GNPH07] is a decomposition of the vertices of Σ into 0-, 1-, 2- and 3-cells of the Morse complexes of f. Algorithms in [EHNP03, EJ09] produce 3-, 2-, 1- and 0-cells of the Morse and Morse-Smale complexes composed of tetrahedra, triangles, edges and vertices of Σ, respectively. The output of the algorithms based on Forman theory [KKM05, GBHP08, RWS11] (Forman gradient vector field V) can be used to obtain also the decomposition of the underlying mesh K into descending cells associated with critical cells of V. Each descending cell of a critical i-cell σ is composed of all i-cells of K that are reachable by tracing gradients paths of V starting from the boundary of σ. The algorithms in [GBHP08, ČomićDI10] produce the graph encoding the connectivity of Morse and Morse-Smale complexes. In [GBHP08], an algorithm based on Forman theory has been developed to obtain the nodes and arcs of the graph. The algorithm in [ČomićDI10] obtains the graph starting from any segmentation of the tetrahedra of Σ in descending and ascending 3-cells of the Morse complexes of f.

5.1 A Watershed-Based Approach for Building the Morse Incidence Graph

In [ČomićDI10], a two-step algorithm is described for the construction of the Morse incidence graph of a scalar field f, defined on the vertices of a simplicial complex Σ with a manifold carrier. The first step is the decomposition of Σ in descending and ascending n-cells of the Morse complexes. In [ČomićDI10], this decomposition is obtained by extending the well-known watershed algorithm based on simulated immersion from image processing to n-dimensional manifold simplicial meshes [VS91]. The first step of the algorithm is, thus, dimension-independent. The second step of the algorithm, developed for the 2D and 3D cases, consists of the construction of the Morse incidence graph.

The watershed algorithm by simulated immersion has been introduced in [VS91] for segmenting a 2D image into regions of influence of minima, which correspond to ascending 2-cells. We describe the extension of this algorithm from images to scalar fields defined at the vertices of a simplicial mesh in arbitrary dimension. The vertices of the simplicial mesh Σ are sorted in increasing order with respect to the values of the scalar field f, and are processed level by level in increasing order of function values. For each minimum m, an ascending region $A(m)$ is iteratively constructed through a breadth-first traversal of the 1-skeleton of the simplicial mesh Σ (formed by its vertices and edges). For each vertex p, its adjacent, and already processed, vertices in the mesh are examined. If they all belong to the same ascending region $A(m)$, or some of them are watershed points, then p is marked as belonging to $A(m)$. If they belong to two or more ascending regions, then p is marked as a watershed point. Vertices that are not connected to any previously processed vertex are new minima and they start a new ascending region.

Each maximal simplex σ (an n-simplex if we consider an n-dimensional simplicial mesh) is assigned to an ascending region based on the labels of its vertices. If all vertices of σ, that are not watershed points, belong to the same region $A(m)$, then σ is assigned to $A(m)$. If the vertices belong to different ascending regions $A(m_i)$, then σ is assigned to the region corresponding to the lowest minimum.

Descending regions associated with maxima are computed in a completely similar fashion.

The algorithm proposed in [ČomićDI10] for the construction of the Morse incidence graph of f works on a segmentation produced by the watershed algorithm, although any other segmentation algorithm can be used. In the (dimension-independent) preprocessing step, for each descending region in Γ_d, a maximum node in the incidence graph is created, and for each ascending region in Γ_a, a minimum node is created. The algorithm for the construction of saddle nodes is based on inspecting the adjacencies between the regions corresponding to maxima and minima, and is developed for the 2D and the 3D case.

In the 2D case, after the preprocessing step, two steps are performed: (i) creation of the nodes corresponding to saddles, and (ii) creation of the arcs of the incidence graph. To create the saddle nodes, 1-cells of the ascending (or of the descending) complex need to be created. Each 1-cell is a chain of edges of the triangle mesh. Each edge e of Σ is inspected, and is classified with respect to such chain of edges based on the labels of the ascending regions to which the two triangles separated by e belong. Each connected component of edges separating two ascending regions is subdivided into topological 1-cells. Thus, if necessary, new saddle nodes are created. Each saddle node (1-cell) p is connected to the two minima it separates. The arcs between saddle nodes and nodes corresponding to maxima are created by inspecting the endpoints of the 1-cells. Three cases are distinguished, illustrated in Figure 9: if the endpoints of 1-cell p are two maxima, the saddle node corresponding to p is connected to those maxima. If one of the endpoints is not a maximum, a new maximum is created and connected to the saddle. If there is a maximum inside 1-cell p, p is split in two 1-cells, each of which with that maximum as endpoint. If there is some maximum q not connected to any saddle, then that maximum must be inside some 2-cell in Γ_a. In this case, a 1-saddle is created by looking at the 2-cells corresponding to q and at its adjacent 2-cells in Γ_d.

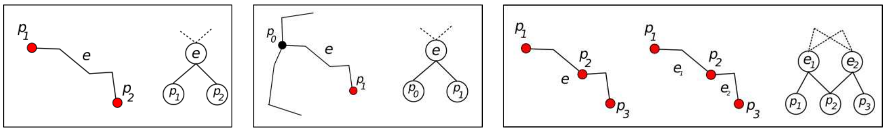

(a) (b) (c)

Fig. 9 Connection of the saddle nodes with maxima in 2D: (a) both endpoints of the 1-cell are maxima; (b) one of the endpoints is not a maximum; (c) there is a maximum in the interior of the 1-cell.

The construction of the Morse incidence graph in 3D requires, after the preprocessing, other three steps, namely, (i) generation of the nodes corresponding to 1-saddles and 2-saddles, (ii) generation of the arcs between 1-saddles and minima, and between 2-saddles and maxima, and (iii) generation of the arcs joining 1- and 2-saddles. The first two steps directly generalize the 2D algorithm. The third step consists of generating the arcs connecting the nodes corresponding to 1-saddles to those corresponding to 2-saddles. For each 2-cell s_1 in Γ_a (which corresponds to a 1-saddle), the set M_s of maxima connected to s_1 is considered, which correspond to the vertices of 2-cell s_1. For each pair of maxima m_1 and m_2 in M_s, it is verified if there exists a 2-cell s_2 (i.e., a 2-saddle) in the descending complex Γ_d between the 3-cells corresponding to m_1 and m_2. If s_2 exists, then the two nodes corresponding to 1-saddle s_1 and 2-saddle s_2 are connected in the MIG. The third step of the algorithm is illustrated in Figure 10. A technique for processing 2-cells which are on the boundary of Σ has been also developed; it is not described here for the sake of brevity.

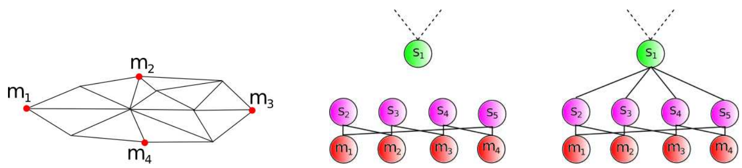

(a) (b) (c)

Fig. 10 Connection of the 1-saddle and 2-saddle nodes in 3D: (a) maxima on the boundary of ascending 2-cell of 1-saddle s_1; (b) 2-saddles s_2, s_3, s_4 and s_5 connected to two maxima on the boundary of the 2-cell; (c) these 2-saddles are connected to 1-saddle s_1.

In summary, the algorithm in [ČomićDI10] is organized in two steps: segmentation of the simplicial mesh Σ into Morse complexes, and extraction of the incidence graph. The first step is dimension-independent. It is based on the extension of a watershed algorithm for intensity images to scalar fields defined on simplicial complexes in arbitrary dimension. The second step, developed for the 2D and 3D cases, constructs the nodes and arcs of the *MIG* encoding the Morse complexes generated at the first step.

5.2 A Boundary-Based Algorithm

The algorithm proposed in [EHNP03] builds a quasi-Morse-Smale complex (see Section 2), a complex that reflects the combinatorial structure of the Morse-Smale complex, but in which the arcs and quadrangles (1- and 2-cells) may not be those of maximal ascent and descent. The quasi-Morse-Smale complex is constructed during two sweeps over a simplicial complex Σ triangulating a 3-manifold M. The first sweep (in the direction of decreasing function value) computes the descending 1- and 2-cells and the second sweep (in the direction of increasing function value) the ascending 1- and 2-cells of the Morse complexes. The algorithm is boundary-based, as it computes the 1- and 2-cells which bound the 3-cells in the Morse complexes. During the first sweep, the descending 1-cells and 2-cells are computed simultaneously. A 1-cell is built as follows:

- If a current vertex p in the sweep is a 1-saddle, a descending 1-cell is started. The two arcs of the corresponding 1-cell are initialized by edges from p to the lowest vertex in each connected component of the lower link of p, as illustrated in Figure 11 (a).
- If there is a descending arc ending at a current vertex p, it is expanded by adding an edge from p to the lowest vertex in its lower link. If p is a 1-saddle, later an ascending 2-cell will start at p and each descending arc is extended to the lowest vertex in the specific connected component of the lower link of p that is not separated from the arc by the ascending 2-cell.
- If p is a minimum, it becomes a node of the Morse-Smale complex, and the descending arcs end at p.

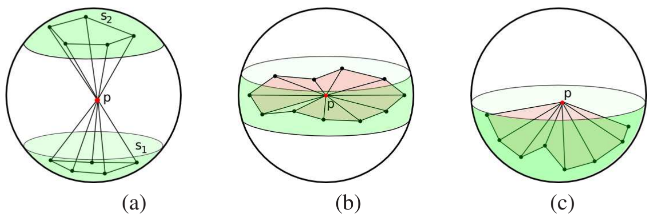

Fig. 11 (a) The 1-cell associated with 1-saddle p is initialized by connecting p to the two lowest vertices s_1 and s_2 in its lower link in [EHNP03]. (b) The 2-cell associated with a 2-saddle p is initialized by the triangles determined by p and a cycle of edges in the lower link of p in [EHNP03]. (c) Expanding a separating 2-cell at a regular vertex p in [EJ09].

A 2-cell is built as follows:

- If a current vertex p in the sweep is a 2-saddle, a descending 2-cell is started. A cycle of edges in the lower link is constructed, which contains the lowest vertex in the lower link of p. Triangles determined by p and edges of the cycle form the initial descending 2-cell of p, as illustrated in Figure 11 (b). Initially, the entire boundary of the descending 2-cell is unfrozen.

- A 2-cell is expanded by constructing a shortest-path tree in the lower link of the current (highest) vertex q on the unfrozen boundary of the 2-cell associated with 2-saddle p, and connecting q to the edges of this tree. If q is a critical point (a 1-saddle or a minimum), it is declared frozen together with its two incident edges on the boundary.
- When the complete boundary of a 2-cell is frozen the 2-cell is completed.

The next step consist of building the intersections between descending and ascending 2-cells by tracing ascending paths inside a descending 2-cell, starting from 1-saddles on the boundary of the descending 2-cell and ending at the 2-saddle that started the descending 2-cell. These intersections are used to guarantee the structural correctness of the extracted quasi-Morse-Smale complex. Each 2-saddle starts two arcs of an ascending 1-cell, which must not cross any already established descending 2-cells. The intersection curves between descending and ascending 2-cells, and the ascending 1-cells decompose each ascending 2-cell into quadrangles. The ascending cells are built one quadrangle at a time, similarly to descending 2-cells.

In summary, the algorithm in [EHZ01] extracts the boundaries of the 3-cells in the Morse-Smale complex. The extracted complex has the correct combinatorial structure described by a quasi-Morse-Smale complex. Each 3-cell in the extracted complex has quadrangular faces.

5.3 A Watershed-Based Labeling Algorithm

In [EJ09], an algorithm is proposed that extracts 3-cells in the descending Morse complex starting from the values of a scalar field f defined over a triangulation Σ of a manifold M. To this aim the algorithm generates two functions on the simplexes of Σ: the *marking function* marks the simplexes of Σ that form the boundaries between descending 3-cells by 1, and the other simplexes of Σ are marked by 0; the *labeling function* labels each simplex σ of Σ marked by 0 by the label of the maximum whose descending 3-cell contains σ. The vertices are inspected in decreasing order of function value. Depending on the type of criticality of a current vertex p, the lower star of p (defined by p and simplexes in the lower link $Lk^-(p)$ of p) is processed.

- If p is a maximum, its lower link is equal to its link. Vertex p starts a new descending 3-cell. All simplexes in the lower star of p are labeled by the label of this 3-cell.
- If p is a regular point (see Figure 11 (c)), its lower link is a deformation retract of a disk. If there is a separating 2-cell that reached p, it is extended across p by creating a spanning tree in the lower link of p. The spanning tree is constructed so that it contains all vertices that belong to an already marked simplex (i.e., to a simplex which is part of the boundary between two descending 3-cells). All triangles and edges connecting p to this spanning tree are marked (extending a descending 2-cell between two 3-cells). Other non-labeled (and non-marked) simplexes in the star of p are labeled by copying from the neighbors. Otherwise

(if there is no separating 2-manifold containing p), non-labeled simplexes in the star of p are labeled by copying from neighbors.

- If p is a 1-saddle, its lower link has two components, each a deformation retract of a disk. Each component of the lower link of p is processed in the same way as in the case of a regular point.
- If p is a 2-saddle, its lower link is a deformation retract of an annulus. Vertex p starts a new separating 2-cell. A cycle that encircles the whole lower link of p is created. All triangles and edges connecting p to this cycle are marked. They form the initial separating 2-cell associated with p. Other non-labeled simplexes in the star of p are labeled by copying from neighbors.
- If p is a minimum, its lower link is empty, and p is marked.

The descending 3-cells of maxima produced by the algorithm in [EJ09] are topological cells.

5.4 A Region-Growing Algorithm

The algorithm proposed in [GNPH07] computes the Morse-Smale complex of a function f defined over the vertices of a simplicial complex Σ triangulating a manifold M. The ascending cells are computed through region growing, in the order of decreasing cell dimension. Descending cells are computed inside the ascending 3-cells, using the same region-growing approach. The ascending and descending cells of all dimensions are composed of vertices (0-simplexes) of Σ.

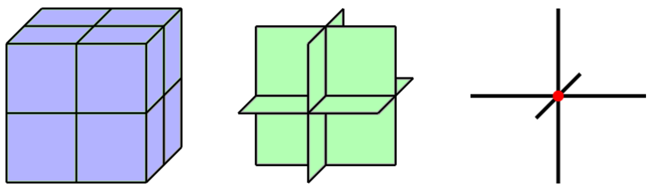

(a) (b) (c)

Fig. 12 Classification of the vertices of Σ as internal or boundary. (a) All the vertices are classified as internal to a 3-cell (blue) with the exception of vertices on the boundary of two or more 3-cells, which are classified as boundary. (b) The boundary vertices in (a) are classified again as internal (green) or boundary for 2-cells. (c) The boundary vertices of the 1-cells in (b) is classified as maxima (red).

The computation of the ascending 3-cells consists of two steps. First, the set of minima of f are identified. Each minimum will be the origin for a set of vertices representing an ascending 3-cell. Then, each vertex p of Σ is classified as an internal vertex of an ascending cell, or as a boundary vertex. This depends on the number of connected components of the set of internal vertices in the lower link of p which are already classified as interior to some ascending 3-cell (see Figure 12 (a)). The classification is performed by sweeping Σ in the order of ascending function values.

Vertices classified as boundary in the first step of the algorithm are the input for the algorithm which builds the ascending 2-cells. An ascending 2-cell is created for each pair of adjacent 3-cells. The vertices of the 2-cells are classified as interior or boundary, based on local neighborhood information, similarly to the classification with respect to the 3-cells (see Figure 12 (b)). A 1-cell is created in every place where ascending 2-cells meet. Each 1-cell is composed of vertices classified as boundary in the previous step. Finally, each vertex p of an ascending 1-cell is classified as interior or boundary. Maxima are created at the boundaries between ascending 1-cells (see Figure 12 (c)). They form a small disjoint clusters of vertices.

For each ascending n-cell, the descending cells are computed in their interior. The region-growing steps are the same. Again here, iteration is performed in the order of decreasing dimension.

The main characteristics of the algorithm in [GNPH07] is that all the cells in the computed Morse complexes are composed of vertices of the simplicial mesh Σ. These cells are computed iteratively in order of decreasing dimension.

5.5 An Algorithm Based on Forman Theory

The algorithm proposed in [GBHP08] computes the Morse-Smale complex starting from a regular n-dimensional CW-complex K with scalar field f defined at the vertices of K. Intuitively, a (finite) CW complex is a finite collection of pairwise disjoint cells, in which the boundary of each cell is the disjoint union of cells of lower dimension. Function f is extended to a Forman function F, defined on all cells of K, such that $F(\sigma)$ is slightly larger than $F(\tau)$ for each cell σ and each face τ of σ. For the defined Forman function F, all cells of K are critical. A discrete gradient vector field is computed by assigning gradient arrows in a greedy manner in ordered sweeps over the cells of K according to increasing dimension and increasing F value. Each current non-paired and non-critical cell in the sweep is paired with its co-facet with only one facet not marked (as critical or as already paired). If there are several of such co-facets the lowest is taken. If there is no such co-facet, a cell cannot be paired, and it is critical. This pairing defines a discrete gradient vector field, as illustrated in Figure 13 (a).

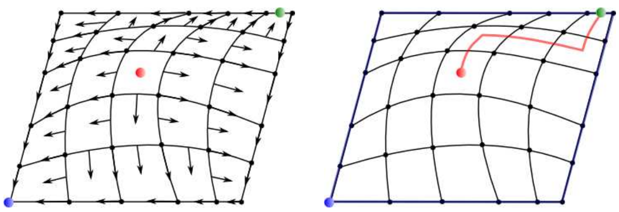

(a) (b)

Fig. 13 (a) Construction of the Forman gradient vector field, and (b) of the incidence graph.

The 1-skeleton of the Morse-Smale complex is computed starting from this gradient vector field. Critical cells of F (and not critical points of f) and the discrete gradient paths connecting them determine the nodes and arcs in the 1-skeleton of the Morse-Smale complex (incidence graph), as illustrated in Figure 13 (b). In [GP12], this algorithm has been extended to extract topological 2- and 3-cells from a regular hexahedral 3D mesh.

The order in which the cells in K are processed by the algorithm is not completely deterministic, since there could be many different i-cells in K with the same value of function F. As a consequence, some unnecessary critical cells may be produced by the algorithm.

5.6 A Forman-based Approach for Cubical Complexes

In [RWS11], a dimension-independent algorithm is proposed for constructing a Forman gradient vector field on a cubical complex K with scalar field values given at the vertices, and applications to the 2D and 3D images are presented.

The algorithm processes the lower star of each vertex v in K independently. For each cell σ in the lower star, the value $\max_{p\in\sigma} f(p) = fmax(\sigma)$ is considered. An ascending order Δ is generated based on the values $fmax(\sigma)$ and the dimension of σ, such that each cell σ comes after its faces in the order. If the lower star of vertex v is v itself, then v is a local minimum and it is added to the set C of critical cells. Otherwise, the first edge e in Δ is chosen and vertex v is paired with edge e (the vector field V at v is defined as $V(v) = e$).

The star of v is processed using two queues, *PQone* and *PQzero*, corresponding to i-cells with one and zero unpaired faces, respectively. All edges in the star of v different from e are added to *PQzero*. All cofaces of e are added to *PQone* if the number of unpaired faces is equal to one.

If queue *PQone* is not empty, the first cell α is removed from the queue. If the number of unpaired faces of α has become zero, α is added to *PQzero*. Otherwise, the vector field at the unique unpaired face $pair(\alpha)$ of α is defined as $V(pair(\alpha)) = \alpha$, $pair(\alpha)$ is removed from *PQzero* and all the co-faces of either α or $pair(\alpha)$ and with number of unpaired faces equal to one are added to *PQone*.

If *PQone* is empty and *PQzero* is not empty, one cell β is taken from *PQzero*. Cell β is added to the set C of critical points and all the co-faces of β with number of unpaired faces equal to one are added to *PQone*.

If both *PQzero* and *PQone* are empty, then the next vertex is processed. Result of the algorithm is the set C of critical cells and the pairing of non-critical cells, which define the Forman gradient vector field V.

In Figure 14 we show the main steps of the algorithm in [RWS11] when processing the lower star of vertex 9 (see Figure 14 (a)). Each vertex is labeled by its scalar field value. Other cells are labeled by the lexicographic order Δ. The lower star of 9 is not 9 itself, and thus 9 is not a minimum. The lowest edge starting from 9 (edge 92), is chosen to be paired with 9. All the other edges are inserted in *PQzero* and the cofaces of 92 with a single unpaired face (faces 9432 and 9852) are inserted in *PQone* (Figure 14 (b)). The first face is taken from *PQone* (face 9432) and coupled with its single unpaired face (edge 94). The face 9741, which is a coface of 94 with exactly one unpaired face, is inserted in *PQone* and edge 94 is removed from *PQzero* (Figure 14 (c)). Face 9741 is taken from *PQone* and paired with edge 97,

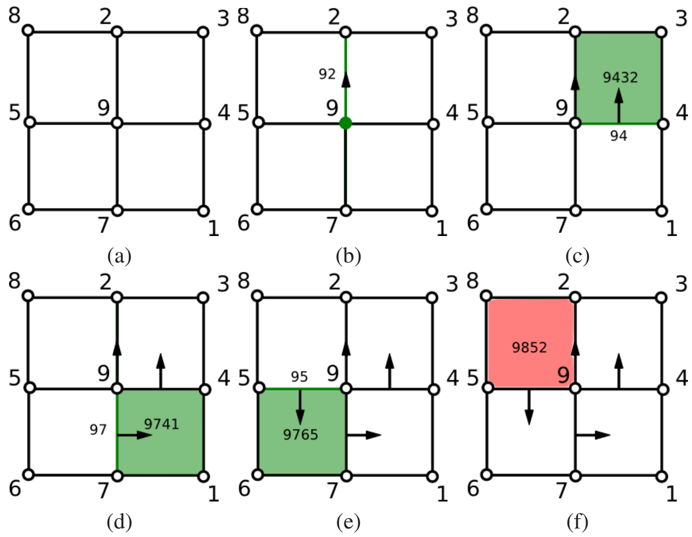

Fig. 14 Processing the lower star of vertex 9 using the algorithm in [RWS11].

which is removed from *PQzero*. Face 9765 is inserted in *PQone* and successively removed to be paired with edge 95 (Figure 14 (d) and (e)). Face 9852 is removed from *PQone* and declared critical, as it has no unpaired faces (Figure 14 (f)).

In the 3D case, the algorithm in [RWS11] does not create spurious critical cells. The extracted critical cells are in a one-to-one correspondence with the changes in topology in the lower level cuts of cubical complex K.

5.7 A Forman-based Approach for Simplicial Complexes

The algorithm proposed in [KKM05] takes as input a scalar field f defined over the vertices of a 3D simplicial complex Σ and a persistence value $p \geq 0$. It computes a Forman gradient vector field V by subdividing the simplexes of Σ into three lists, denoted as A, B and C, such that lists A and B are of the same length, and for each i-simplex $\sigma_j \in A$, $V(\sigma_j) = \tau_j$, τ_j is the $(i+1)$-simplex in B, and C is the set of critical simplexes.

The algorithm builds the Forman gradient vector field in the lower link $Lk^-(v)$ of each vertex v in Σ, and extends this field to the cone $v * Lk^-(v)$. Lists A, B and C are initialized as empty. For each vertex v in Σ, if $L(v)$ is empty, then v is a minimum and it is added to C. Otherwise, v is added to A and the algorithm is recursively called on the lower link $L^-(v)$, producing lists A', B', C' that define the Forman gradient vector field V' on $Lk^-(v)$. The lowest critical vertex w is chosen from C' and edge $[v,w]$ is added to B. Thus, $V(v) = [v,w]$. For each i-simplex σ (different from w) in C' the $(i+1)$-simplex (cone) $v * \sigma$ is added to C. For each i-simplex σ in A' the $(i+1)$-simplex $v * \sigma$ is added to A and the $(i+2)$-simplex $v * V'(\sigma)$ is added to B. Thus, $V(v * \sigma) = v * V'(\sigma)$.

Once all the lower links of vertices in Σ have been processed, a *persistence canceling step* is performed in increasing order of dimension i. For each critical i-simplex σ, all the gradient paths to critical $(i-1)$-simplexes are found. A critical i-simplex σ can be cancelled with critical $(i-1)$-simplex γ if and only if there is only one gradient path from σ to γ. The effect of a cancellation is to reverse the gradient path connecting σ and γ. Cancellations are applied in the order of increasing persistence. The function that extends the scalar field f to the simplexes of Σ, and whose values are considered in the definition of persistence, is given by $fmax(\sigma) = \max_{p \in \sigma} f(p)$.

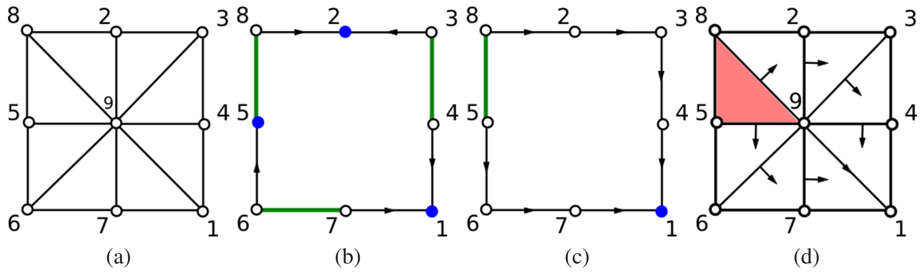

Fig. 15 (a) The lower star of vertex 9. The Forman gradient vector field V' on the link of 9 (b) before and (c) after the cancellation of critical edge [4,3] and vertex 2, and edge [7,6] and vertex 5. The critical vertices are blue, and the critical edges are green. (d) The Forman gradient vector field V in the lower star of vertex 9.

We illustrate the algorithm in [KKM05] in Figure 15. The star of vertex 9 is shown in Figure 15 (a). The application of the algorithm to the lower link $Lk^-(9)$ of vertex 9 produces the following lists:

A' $= 3;4;6;7;8$

B' $= [3,2];[4,1];[6,5];[7,1];[8,2]$

C' $= 1;2;[4,3];5;[7,6];[8,5]$

The corresponding Forman gradient vector field V' on $Lk^-(9)$, and V' after the cancellation of vertex 2 and edge [3,4], and cancellation of vertex 5 and edge [6,7], are shown in Figure 15 (b) and (c), respectively. The extension of V' to the cone $9 * Lk^-(9)$ (the lower star of vertex 9) is shown in Figure 15 (d). Descending and ascending regions of critical cells of Forman vector field V constructed in [KKM05] are computed in [JMK09].

If Σ is a triangulation of a 3D manifold and the scalar field f defined at the vertices of Σ has no multiple saddles, then there is a critical i-cell of the computed Forman gradient vector field V for each i-saddle of the scalar field f.

5.8 Analysis and Comparison

We have described seven algorithms for extracting Morse or Morse-Smale complexes of a scalar field f in the discrete case. We summarize the properties of the reviewed algorithms in Table 1.

Algorithm	Input	Dimension	Approach	Critical points	Morse cells
[ČomićDI10]	simplicial	3D	region	extrema	simplexes of Σ
[EHNP03]	simplicial	3D	boundary	all	simplexes of Σ
[EJ09]	simplicial	3D	boundary	all	simplexes of Σ
[GNPH07]	simplicial	3D	region	extrema	vertices of Σ
[GBHP08]	CW	nD	Forman	critical cells	cells of K
[RWS11]	cubical	nD	Forman	critical cells	cells of K
[KKM05]	simplicial	3D	Forman	critical cells	cells of Σ

Table 1 Reviewed algorithms classified according to the type of the input complex (simplicial or cell), dimension of the complex, approach used (region-based, boundary-based or based on Forman theory), type of extracted critical entities (critical points of the given scalar field f or critical cells of the constructed Forman gradient vector field V) and type of entities that form the extracted cells in the Morse complexes (cells or vertices of the input complex).

We can classify the reviewed algorithms based on different criteria. All algorithms work on a 3D manifold simplicial complex Σ except the ones in [GBHP08, RWS11], which work on an arbitrary-dimensional CW-complex and cubical complex, respectively.

With respect to the approach used, some of the algorithms we reviewed [ČomićDI10, GNPH07] can be classified as region-based, as they extract 3-cells corresponding to extrema. Others [EHNP03, EJ09] are boundary based, as they extract the boundaries between the 3-cells corresponding to extrema. The algorithms in [GBHP08, RWS11, KKM05] compute a Forman gradient vector field V starting from scalar field f.

The algorithms differ also in the type of critical points they extract before producing the segmentation of the input mesh: some algorithms [EHNP03, EJ09] first classify all critical points of scalar field f (extrema and saddles); others [ČomićDI10, GNPH07] extract only extrema of f, and obtain the other nodes in the Morse incidence graph from the adjacency relation between 3-cells associated with extrema. The algorithms in [GBHP08, RWS11, KKM05] extract the critical cells of a Forman gradient vector field V (and not the critical points of scalar field f) defined through f.

Finally, another difference among the algorithms is given by the entities used in the segmentation process: the algorithms in [ČomićDI10, EHNP03, EJ09] assign the simplexes of Σ to cells in the Morse complexes; the algorithm in [GNPH07] assigns the vertices of Σ to cells in the Morse complexes; the algorithms in [GBHP08, RWS11, KKM05] assign the cells of the cell complex K to cells in the descending Morse complex.

The algorithm in [EHZ01] computes the segmentation of the 3D simplicial mesh with the correct combinatorial structure described by the quasi-Morse-Smale complex. The algorithm in [EJ09] produces 3-cells in the descending Morse complex, which are topological cells. In the 3D case, the algorithm in [RWS11] computes the critical cells of the Forman gradient vector field V that are in a one-to-one correspondence with the changes in topology in the lower level cuts of K. If Σ is a triangulation of a manifold M, and scalar field f has no multiple saddles, then the algorithm in [KKM05] produces a critical i-cell of the Forman gradient vector field for each i-saddle of scalar field f. There are no formal claims about the critical cells of Forman gradient vector field computed by the algorithm in [GNPH07].

6 Simplification of 3D Morse and Morse-Smale Complexes

Although Morse and Morse-Smale complexes encode compactly the behavior of a scalar field f and the topology of its domain, simplification of these complexes is an important issue for two major reasons. The first is the over-segmentation (the presence of a large number of small and insignificant regions) produced by Morse and Morse-Smale complexes which is due to the presence of noise in the data sets, both in case they are obtained through measurements or as a result of a simulation algorithm. Simplification of the complexes through elimination of pairs of critical points can be used to eliminate noise. Each simplification is performed guided by *persistence*, which measures the importance of the pair of eliminated critical points, and is equal to the absolute difference in function values between them. Usually by using a threshold on persistence equal to 5%-10% of the maximum persistence value, a reduction of the storage cost in the representation of the Morse or Morse-Smale complexes can be obtained which amounts to 10%-20% for 2D data sets, and 5%-10% for 3D ones.

Even after a simplification which removes insignificant regions considered to be noise, and leaves regions that correspond to actual features of the scalar field, the size of Morse and Morse-Smale complexes can still be large, due to the huge size and amount of available scientific data. Thus, the second requirement is to reduce the size of the complexes at different levels of resolution, while retaining information on important structural features of the field and guaranteeing the topological correctness of the simplified representations. The size of a Morse complex is about 0.4%-3% the size of the underlying simplicial mesh in 2D and about 2%-8% in 3D. For large 3D data sets (which have 15M tetrahedra), the size of a Morse complex can be up to 50 MBytes.

We describe here two approaches to the simplification of Morse and Morse-Smale complexes in 3D proposed in the literature. The first approach [GNP$^+$05] applies the *cancellation* operator of critical points of a Morse function f [Mat02] on the Morse-Smale complexes of f. The second approach [ČomićD11] applies a new set of simplification operators, called *removal* and *contraction*, which, together with their inverse refinement ones, form a minimally complete basis of operators for performing any topologically consistent simplification on Morse and Morse-Smale complexes.

Both cancellation and removal/contraction operators eliminate a pair of critical points of scalar field f, i.e., a pair of cells in the Morse complexes and a pair of vertices from the Morse-Smale complex. The difference between the two approaches to simplification is that cancellation often introduces a large number of cells (of dimension higher than zero) in the Morse-Smale complex, while this never happens with removal/contraction. Cancellation operator applied on large data sets can create complexes that exceed practical memory capabilities [GBHP11]. Removal/contraction operator, on the other hand, reduces the size of the complexes at each step of the simplification process.

6.1 Cancellation in 3D

In this section, we review the cancellation operator, which simplifies a Morse function f defined on a manifold M by eliminating its critical points in pairs [Mat02]. Two critical points p and q can be cancelled if

1. p is an i-saddle and q is an $(i+1)$-saddle, and
2. p and q are connected through a unique integral line of f.

After the cancellation of p and q, each critical point t of index at least $i+1$, which was connected through integral line of f to i-saddle p becomes connected to each critical point r of index at most i, which was connected to $(i+1)$-saddle q before the cancellation. Equivalently, in a descending (and, symmetrically, ascending) Morse complex, an i-cell p and an $(i+1)$-cell q can be simultaneously cancelled if cell p appears exactly once on the boundary of cell q. After the cancellation, each cell r which was on the boundary of $(i+1)$-cell q becomes part of the boundary of each cell t which was in the co-boundary of i-cell p. In the Morse-Smale complex, there is a new k-cell for each two cells t and r that become incident to each other in the Morse complexes after the cancellation and that differ in dimension by k.

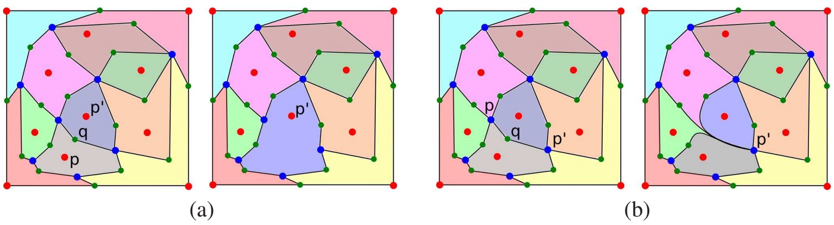

Fig. 16 (a) Cancellation of a maximum p and saddle q, and (b) cancellation of a minimum p and a saddle q, on the 2D descending Morse complex illustrated in Figure 2 (a).

In 2D, there are two cancellation operators: cancellation of a maximum and a saddle, and cancellation of a minimum and a saddle. A cancellation of a maximum p and a saddle q is illustrated in Figure 16 (a). It is feasible if 1-cell q is shared by exactly two 2-cells p and p'. After the cancellation, 1-cell q (corresponding to saddle) is deleted, and 2-cell p (corresponding to maximum) is merged into 2-cell p'. A cancellation of a minimum p and a saddle q is illustrated in Figure 16 (b). It is feasible if 1-cell q is bounded by two different 0-cells p and p'. After the cancellation, 1-cell q is deleted, and 0-cell p is collapsed onto 0-cell p'.

In 3D, there are two instances of a cancellation: one cancels an extremum and a saddle (a maximum and a 2-saddle, or a minimum and a 1-saddle), the other cancels two saddle points. Cancellation of a maximum p and a 2-saddle q is feasible if 2-cell q is shared by exactly two different 3-cells p and p'. In the descending Morse complex, it removes 2-cell q, thus merging 3-cell p into 3-cell p', as illustrated in

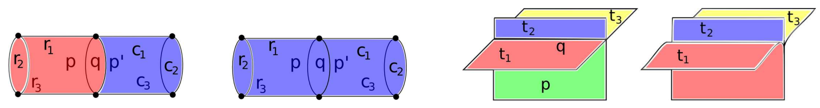

(a) (b)

Fig. 17 Portion of a 3D descending Morse complex before and after (a) a cancellation of maximum p and 2-saddle q, and (b) a cancellation of a 1-saddle p and 2-saddle q.

Figure 17 (a). Cancellation of a minimum p and a 1-saddle q is feasible if 1-cell q is bounded by exactly two different 0-cells p and p'. In the descending complex Γ_d, it contracts 1-cell q with the effect of collapsing 0-cell p on 0-cell p'.

Cancellations that do not involve an extremum are more complex. The problem is that the number of cells in the Morse complexes that become incident to each other (and thus, the number of cells in the Morse-Smale complex) may increase after a cancellation. Let p and q be a 1-saddle and a 2-saddle, respectively. Let $R = \{r_j, j = 1,..,j_{max}\}$ be the set of 2-saddles connected to p and different from q, and let $T = \{t_k, k = 1,..,k_{max}\}$ be the set of 1-saddles connected to q different from p. The effect of the cancellation of 1-saddle p and 2-saddle q on a 3D descending Morse complex is illustrated in Figure 17 (b). 1-cell p and 2-cell q are deleted, and the boundary of each 2-cell in R incident in p is extended to include 1-cells in T on the boundary of 2-cell q. Each 1-cell and each 0-cell that was on the boundary of 2-cell q (with the exception of 1-cell p) becomes part of the boundary of each 2-cell and each 3-cell incident in p (with the exception of 2-cell q), thus increasing the incidence relation on the descending Morse complex. The effect of the cancellation on the Morse-Smale complex consists of adding one arc for each pair (r_j, t_k) of critical points, where r_j belongs to R and t_k belongs to T, and deleting p and q, as well as all the arcs incident in them. Thus, a cancellation of p and q increases the number of arcs connecting 1-saddles to 2-saddles in the complex by deleting $|R| + |T| + 1$ such arcs, but adding $|R| \cdot |T|$ arcs. Similarly, the number of 2-cells and 3-cells in the Morse-Smale complex may increase after the cancellation.

In [GNP$^+$06], a macro-operator is defined, which consists of a 1-saddle-2-saddle cancellation, followed by a sequence of cancellation involving extrema. These latter cancellations eliminate the new incidences in the Morse complexes, the new cells in the Morse-Smale complex, and the new arcs in the incidence graph.

6.2 Removal and Contraction Operators

Motivated by the fact that cancellation operator is not a real simplification operator, two new basic dimension-independent simplification operators are introduced [ČomićD11], called *removal* and *contraction*. They are defined by imposing additional constraints on the feasibility of a cancellation, and can be seen as merging of cells in the Morse complexes. There are two types of both a removal and contraction operator. For simplicity, we describe only the 3D instances of the operators of the first type.

A removal $rem(p,q,p')$ of index i of the first type of $(i+1)$-cell p and i-cell q is feasible if i-cell q appears once on the boundary of exactly two different $(i+1)$-cells p and p'. Intuitively, a removal $rem(p,q,p')$ removes i-cell q and merges $(i+1)$-cell p into $(i+1)$-cell p' in the descending Morse complex Γ_d. In the dual ascending Morse complex Γ_a, it contracts $(n-i)$-cell q and collapses $(n-i-1)$-cell p onto $(n-i-1)$-cell p'.

In 2D, there is one removal operator (of index 1). It is the same as a cancellation of a maximum and a saddle, illustrated in Figure 16 (a).

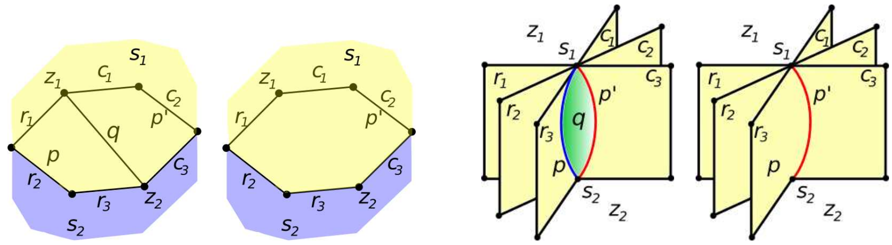

(a) (b)

Fig. 18 Portion of a 3D descending (a) and ascending (b) Morse complex before and after a removal $rem(p,q,p')$ of index 1. The boundary of 2-cell p, consisting of 1-cells r_1, r_2 and r_3, is merged into the boundary of 2-cell p' in Γ_d. The co-boundary of 1-cell p, consisting of 2-cells r_1, r_2 and r_3, is merged into the co-boundary of 1-cell p' in Γ_a.

In 3D, there are two removal operators: a removal of index 1 of 1-saddle q and 2-saddle p, and a removal of index 2 of 2-saddle q and maximum p. This latter is the same as the maximum-2-saddle cancellation illustrated in Figure 17 (a).

A removal $rem(p,q,p')$ of index 1 in 3D is different from a cancellation, since it requires that 1-cell q bounds exactly two 2-cells p and p' in the descending complex. An example of the effect of a removal $rem(p,q,p')$ of index 1 on a 3D descending Morse complex is illustrated in Figure 18 (a). After the removal, in the simplified descending Morse complex Γ_d', 1-cell q is deleted, and 2-cell p is merged with the unique 2-cell p' in the co-boundary of q and different from p. The boundary of p becomes part of the boundary of p'. Figure 18 (b) illustrates the effect of removal $rem(p,q,p')$ on the dual ascending complex Γ_a. In Γ_a, q is a 2-cell bounded by exactly two different 1-cells p and p'. After the removal, 2-cell q is contracted, 1-cell p is collapsed onto 1-cell p'. All cells in the co-boundary of p become part of the co-boundary of p'.

Contraction operators are dual to removal operators. The effect of a contraction of index i on a descending complex Γ_d is the same as the effect of a removal of index $(n-i)$ on an ascending complex Γ_a. Figure 18 (b) and (a) illustrates the effect of a contraction $con(p,q,p')$ of index 2 on a descending and ascending Morse complex, respectively, and thus also the duality between removal and contraction operators.

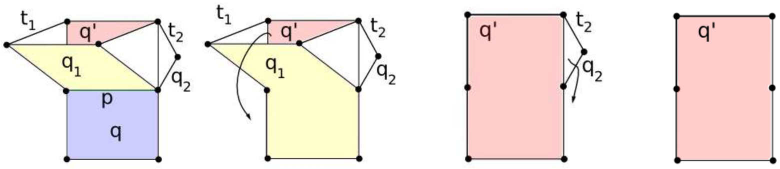

Fig. 19 A sequence consisting of a cancellation of 1-saddle p and 2-saddle q, followed by removals, which eliminate 2-saddles and 3-saddles connected to p, on a 3D descending Morse complex.

In [ČomićD11], it has been shown that removal and contraction simplification operators, together with their inverse ones, form a basis for the set of topologically consistent operators on Morse and Morse-Smale complexes on a manifold M. In particular, the macro-operator defined in [GNP$^+$06], illustrated in Figure 19, which cancels 1-cell p and 2-cell q and eliminates the cells created by this cancellation in the Morse-Smale complex, can be expressed as a sequence of removal and contraction operators, illustrated in Figure 20. 1-cell p is incident to four 2-cells, and 2-cell q is incident to four 1-cells. To be able to apply one of our operators (e.g. a removal of 1-cell p), which will eliminate 1-cell p and 2-cell q, we need to have only two 2-cells q and q' incident to 1-cell p. We can reduce the complex Γ_d to this situation by applying two removals of index 2, until all 2-cells incident to 1-cell p, with the exception of 2-cell q and one other 2-cell q' are eliminated. Now, we can apply a removal $rem(q, p, q')$, which eliminates 1-cell p and 2-cell q. Such sequence of removals consists of the same number of operators as a macro-operator consisting of a sequence of cancellations (macro-1-saddle-2-saddle operator), and it maintains simpler Morse and Morse-Smale complexes at each step.

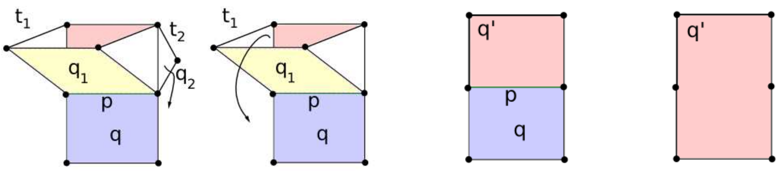

Fig. 20 A sequence consisting of removals, which eliminate 2-saddles and 3-saddles connected to p, followed by a removal of index 1 that eliminates 1-saddle p and 2-saddle q on a 3D descending Morse complex.

We have developed a simplification algorithm on the Morse complexes based on the removal and contraction simplification operators. Simplifications are applied in increasing order of persistence [EHZ01]. Our simplification algorithm can be applied not only to scalar fields representing the elevation, but to any scalar field, such as for example a discrete distortion [WDM10], which generalizes the notion of curvature.

In Figure 21, we illustrate the result of our simplification algorithm on a 3D Bucky Ball data set, depicted in Figure 21 (a), which represents a carbon molecule having 60 atoms arranged as a truncated icosahedron. The full-resolution graph is shown in Figure 21 (b). The incidence graphs after 200 and 400 simplifications are shown in Figure 21 (c) and (d), respectively.

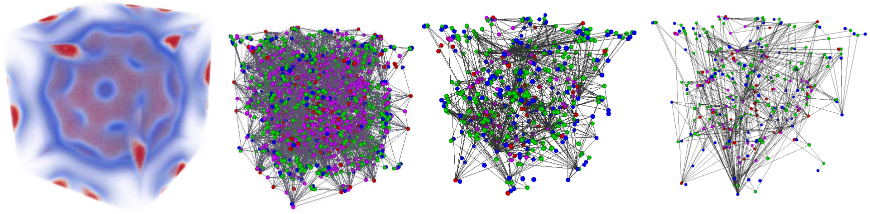

(a) (b) (c) (d)

Fig. 21 (a) Field behavior for the Bucky Ball data set. (b) The incidence graph at full resolution, and the incidence graph after (c) 200 and (d) 400 simplifications.

7 Concluding Remarks

The problem of modeling and simplifying Morse and Morse-Smale complexes in 2D has been extensively studied in the literature. Here, we have reviewed some recent work which extends these results to three and higher dimensions. We have described and compared data structures for representing Morse and Morse-Smale complexes. We have described and compared algorithms for extracting these complexes starting from the values of a scalar field f given at the vertices of a simplicial or a cell complex triangulating a manifold M. Finally, we have described and compared existing simplification operators on Morse and Morse-Smale complexes.

Simplification operators, together with their inverse refinement ones, form a basis for the definition of a multi-resolution model of Morse and Morse-Smale complexes [DČomićI12].

The next challenge is how to extract representations of the geometry of the field which is compatible with the reduced incidence graph extracted from the multiresolution model [DDMV10, BEHP04, WGS10].

Acknowledgements

This work has been partially supported by the Italian Ministry of Education and Research under the PRIN 2009 program, and by the National Science Foundation under grant number IIS-1116747.

References

[Ban70] T. Banchoff. Critical Points and Curvature for Embedded Polyhedral Surfaces. *American Mathematical Monthly*, 77(5):475–485, 1970.

[BEHP03] P.-T. Bremer, H. Edelsbrunner, B. Hamann, and V. Pascucci. A Multi-Resolution Data Structure for Two-Dimensional Morse Functions. In *Proceedings IEEE Visu-*

alization 2003, pages 139–146. IEEE Computer Society, October 2003.

[BEHP04] P.-T. Bremer, H. Edelsbrunner, B. Hamann, and V. Pascucci. A Topological Hierarchy for Functions on Triangulated Surfaces. *Transactions on Visualization and Computer Graphics*, 10(4):385–396, July/August 2004.

[Beu94] S. Beucher. Watershed, Hierarchical Segmentation and Waterfall Algorithm. In *Proc. Mathematical morphology and its Applications to Image Processing*, pages 69–76, 1994.

[BFF+08] S. Biasotti, L. De Floriani, B. Falcidieno, P. Frosini, D. Giorgi, C. Landi, L. Papaleo, and M. Spagnuolo. Describing shapes by geometrical-topological properties of real functions. *ACM Comput. Surv.*, 40:Article 12, 2008.

[BPH05] P.-T. Bremer, V. Pascucci, and B. Hamann. Maximizing Adaptivity in Hierarchical Topological Models. In *Proceedings of International Conference on Shape Modeling and Applications 2005 (SMI '05), Belyaev, A.G., Pasko, A.A. and Spagnuolo, M., eds.*, pages 298–307, Los Alamitos, California, 2005. IEEE Computer Society Press.

[BS98] C. L. Bajaj and D. R. Shikore. Topology Preserving Data Simplification with Error Bounds. *Computers and Graphics*, 22(1):3–12, 1998.

[BWP+10] P.-T. Bremer, G. H. Weber, V. Pascucci, M. S. Day, and J. B. Bell. Analyzing and Tracking Burning Structures in Lean Premixed Hydrogen Flames. *IEEE Trans. Vis. Comput. Graph.*, 16(2):248–260, 2010.

[CCL03] F. Cazals, F. Chazal, and T. Lewiner. Molecular Shape Analysis Based upon the Morse-Smale Complex and the Connolly Function. In *Proceedings of the nineteenth Annual Symposium on Computational Geometry*, pages 351–360, New York, USA, 2003. ACM Press.

[ČomićD11] L. Čomić and L. De Floriani. Dimension-Independent Simplification and Refinement of Morse Complexes. *Graphical Models*, 73(5):261–285, 2011.

[ČomićDI10] L. Čomić, L. De Floriani, and F. Iuricich. Building Morphological Representations for 2D and 3D Scalar Fields. In E. Puppo, A. Brogni, and L. De Floriani, editors, *Eurographics Italian Chapter Conference*, pages 103–110. Eurographics, 2010.

[ČomićMD11] L. Čomić, M. M. Mesmoudi, and L. De Floriani. Smale-Like Decomposition and Forman Theory for Discrete Scalar Fields. In *DGCI*, pages 477–488, 2011.

[DČomićI12] L. De Floriani, L. Čomić, and F. Iuricich. Dimension-Independent Multi-Resolution Morse Complexes. In *Shape Modeling International*, page accepted, 2012.

[DDM03] E. Danovaro, L. De Floriani, and M. M. Mesmoudi. Topological Analysis and Characterization of Discrete Scalar Fields. In T.Asano, R.Klette, and C.Ronse, editors, *Geometry, Morphology, and Computational Imaging*, volume LNCS 2616, pages 386–402. Springer Verlag, 2003.

[DDMV10] E. Danovaro, L. De Floriani, P. Magillo, and M. Vitali. Multiresolution Morse Triangulations. In G. Elber, A. Fischer, J. Keyser, and M.-S. Kim, editors, *Symposium on Solid and Physical Modeling*, pages 183–188. ACM, 2010.

[DDVM07] E. Danovaro, L. De Floriani, M. Vitali, and P. Magillo. Multi-Scale Dual Morse Complexes for Representing Terrain Morphology. In *GIS '07: Proceedings of the 15th annual ACM international symposium on Advances in geographic information systems*, pages 1–8, New York, NY, USA, 2007. ACM.

[DH07] L. De Floriani and A. Hui. Shape Representations Based on Cell and Simplicial Complexes. In *Eurographics 2007, State-of-the-art Report*. September 2007.

[EDP+03] E.Danovaro, L. De Floriani, P.Magillo, M. M. Mesmoudi, and E. Puppo. Morphology-Driven Simplification and Multiresolution Modeling of Terrains. In E.Hoel and P.Rigaux, editors, *Proceedings ACM GIS 2003 - The 11th International Symposium on Advances in Geographic Information Systems*, pages 63–70. ACM Press, 2003.

[EHNP03] H. Edelsbrunner, J. Harer, V. Natarajan, and V. Pascucci. Morse-Smale Complexes for Piecewise Linear 3-Manifolds. In *Proceedings 19th ACM Symposium on Computational Geometry*, pages 361–370, 2003.

[EHZ01] H. Edelsbrunner, J. Harer, and A. Zomorodian. Hierarchical Morse Complexes for Piecewise Linear 2-Manifolds. In *Proceedings 17th ACM Symposium on Computational Geometry*, pages 70–79, 2001.

[EJ09] H. Edelsbrunner and . Harer J. The Persistent Morse Complex Segmentation of a 3-Manifold. In Nadia Magnenat-Thalmann, editor, *3DPH*, volume 5903 of *Lecture Notes in Computer Science*, pages 36–50. Springer, 2009.

[For98] R. Forman. Morse Theory for Cell Complexes. *Advances in Mathematics*, 134:90–145, 1998.

[GBHP08] A. Gyulassy, P.-T. Bremer, B. Hamann, and V. Pascucci. A Practical Approach to Morse-Smale Complex Computation: Scalability and Generality. *IEEE Transactions on Visualization and Computer Graphics*, 14(6):1619–1626, 2008.

[GBHP11] A. Gyulassy, P.-T. Bremer, B. Hamann, and V. Pascucci. Practical Considerations in Morse-Smale Complex Computation. In V. Pascucci, X. Tricoche, H. Hagen, and J. Tierny, editors, *Topological Methods in Data Analysis and Visualization: Theory, Algorithms, and Applications*, Mathematics and Visualization, pages 67–78. Springer Verlag, Heidelberg, 2011.

[GNP+05] A. Gyulassy, V. Natarajan, V. Pascucci, P.-T. Bremer, and B. Hamann. Topology-Based Simplification for Feature Extraction from 3D Scalar Fields. In *Proceedings IEEE Visualization'05*, pages 275–280. ACM Press, 2005.

[GNP+06] A. Gyulassy, V. Natarajan, V. Pascucci, P.-T. Bremer, and B. Hamann. A Topological Approach to Simplification of Three-Dimensional Scalar Functions. *IEEE Transactions on Visualization and Computer Graphics*, 12(4):474–484, 2006.

[GNPH07] A. Gyulassy, V. Natarajan, V. Pascucci, and B. Hamann. Efficient Computation of Morse-Smale Complexes for Three-dimensional Scalar Functions. *IEEE Transactions on Visualization and Computer Graphics*, 13(6):1440–1447, 2007.

[GP12] A. Gyulassy and V. Pascucci. Computing Simply-Connected Cells in Three-DimensionalMorse-Smale Complexes. In R. Peikert, H. Hauser, H. Carr, and R. Fuchs, editors, *Topological Methods in Data Analysis and Visualization: Theory, Algorithms, and Applications*, Mathematics and Visualization, pages 31–46. Springer Verlag, Heidelberg, 2012.

[JMK09] G. Jerše and N. Mramor Kosta. Ascending and Descending Regions of a Discrete Morse Function. *Comput. Geom. Theory Appl.*, 42(6-7):639–651, 2009.

[Kel55] J. L. Kelley. *General Topology*. Princeton, N. J.: Van Nostrand, 1955.

[KKM05] H. King, K. Knudson, and N. Mramor. Generating Discrete Morse Functions from Point Data. *Experimental Mathematics*, 14(4):435–444, 2005.

[LLT04] T. Lewiner, H. Lopes, and G. Tavares. Applications of Forman's Discrete Morse Theory to Topology Visualization and Mesh Compression. *Transactions on Visualization and Computer Graphich*, 10(5):499–508, September-October 2004.

[Mat02] Y. Matsumoto. *An Introduction to Morse Theory*, volume 208 of *Translations of Mathematical Monographs*. American Mathematical Society, 2002.

[Mil63] J. Milnor. *Morse Theory*. Princeton University Press, New Jersey, 1963.

[NGH04] X. Ni, M. Garland, and J. C. Hart. Fair Morse Functions for Extracting the Topological Structure of a Surface Mesh. In *International Conference on Computer Graphics and Interactive Techniques ACM SIGGRAPH*, pages 613–622, 2004.

[NWB+06] V. Natarajan, Y. Wang, P.-T. Bremer, V. Pascucci, and B. Hamann. Segmenting molecular surfaces. *Computer Aided Geometric Design*, 23(6):495–509, 2006.

[Pas04] V. Pascucci. Topology Diagrams of Scalar Fields in Scientific Visualization. In S. Rana, editor, *Topological Data Structures for Surfaces*, pages 121–129. John Wiley & Sons Ltd, 2004.

[RWS11] V. Robins, P. J. Wood, and A. P. Sheppard. Theory and Algorithms for Constructing Discrete Morse Complexes from Grayscale Digital Images. *IEEE Trans. Pattern Anal. Mach. Intell.*, 33(8):1646–1658, 2011.

[TIKU95] S. Takahashi, T. Ikeda, T. L. Kunii, and M. Ueda. Algorithms for Extracting Correct Critical Points and Constructing Topological Graphs from Discrete Geographic Elevation Data. In *Computer Graphics Forum*, volume 14, pages 181–192, 1995.

[VS91] L. Vincent and P. Soille. Watershed in digital spaces: An efficient algorithm based on immersion simulation. *IEEE Transactions on Pattern Analysis and Machine Intelligence*, 13(6):583–598, 1991.

[WDM10] K. Weiss, L. De Floriani, and M. M. Mesmoudi. Multiresolution Analysis of 3D Images Based on Discrete Distortion. In *20th International Conference on Pattern Recognition (ICPR)*, pages 4093 – 4096, August 2010.

[WGS10] T. Weinkauf, Y. I. Gingold, and O. Sorkine. Topology-based Smoothing of 2D Scalar Fields with ^{1}-Continuity. *Comput. Graph. Forum*, 29(3):1221–1230, 2010.

[Wol04] G. W. Wolf. Topographic Surfaces and Surface Networks. In S. Rana, editor, *Topological Data Structures for Surfaces*, pages 15–29. John Wiley & Sons Ltd, 2004.